

**Cell Concentrating and Patterning via Interactions between Electric and
Thermal Fields**

Golak Kunti ^a, Tarun Agarwal ^b, Anandaroop Bhattacharya ^a, Tapas Kumar Maiti ^b
and Suman Chakraborty ^{a*}

^aDepartment of Mechanical Engineering, Indian Institute of Technology Kharagpur,
Kharagpur, West Bengal - 721302, India

^bDepartment of Biotechnology, Indian Institute of Technology Kharagpur, Kharagpur,
West Bengal - 721302, India

**E-mail address* of the corresponding author: suman@mech.iitkgp.ernet.in

Abstract

We demonstrate an AC electrokinetic microfluidic platform which uses interactions between electric field and internally generated Joule heating to induce electrical forces, commonly known as electrothermal forces. The toroidal vortices induced by electrothermal forces transport the suspended cells towards a hotspot site for rapid concentrating and patterning into different designs. The technique employs two parallel plate electrodes and an insulating layer over the bottom electrode. To induce nonuniform thermal field the insulating layer is drilled at the middle. Strong electric field penetrates through the narrow hole and generates highly nonuniform Joule heating, which in turn, generates gradients in electrical properties and induces mobile charges to impose directional fluid flow. The characterization of the trapping process is presented for two different biological objects, *Escherichia coli* bacteria and yeast cell.

1. Introduction

A number of operations, such as trapping, transportation, concentration, re-orientation and sorting of cells have been developed in the clinical and biological fields due to increasing demands of the versatile arrangement of cells into desired patterns.^{1,2} Patterning of biological objects is the fundamental basis of cell-cell interactions, bioprinting, drug development, image-based cell selection etc.³⁻⁹ On the other hand, patterning of cells is widely used to design the biosensors, for cellular cultivation, and for scaffolds to pattern proteins.¹⁰ Therefore, a technique which can manipulate a large number of cells rapidly and accurately is essential in the area of biomedical engineering. Many techniques emerged to address the various operations of cell patterning use various forces, namely mechanical,¹¹ optical,^{12,13} magnetic,¹⁴ electrical^{15,16} forces, etc.

The methods which use electrical force, such as electrophoresis (EP), dielectrophoresis (DEP), electrothermal (ET), etc. show many important features of manipulating cells at microscale since they use the inherent electrical properties of the biological objects without necessitating further labeling.^{17,18} They have the ability to trap the cells with high throughput, high speed and high reliability on a microfluidic chip.^{18,19} DEP has been used widely to manipulate cells in a variety of applications showing many advantages, such as induction of low stress on samples, differentiation between particles of different kinds, etc.^{20,21} However, DEP uses fixed electrodes which limits its application in many cases.²¹ Sometimes, it demands complicated electrodes which need to be fabricated in a small space employing expensive microfabrication methodologies.²² In addition, the effectiveness of this method is restricted to large particle because dielectrophoresis force is proportional to cubic of particle radius.²³ Moreover, difficulties of adhesion of cells on the surface of the electrodes inhibit continuous operation of cell manipulation for a long time.²⁴

In recent years, rapid electrokinetic patterning (REP) has emerged as a noninvasive technique for the manipulation of colloidal particles.²⁵ This technique uses parallel plate electrodes to generate a uniform AC electric field. The system works by the influence of an optical landscape with an infrared laser. Particles can be manipulated dynamically using voltage of 1-20 volts peak-to-peak at a frequency of 1-100 kHz. The aggregated particles can

be patterned, translated over the electrode surface at any location. The system generates a small heated area (diameter $\sim 100\ \mu\text{m}$) on the electrodes using a highly focused laser beam. The nonuniform thermal field and uniform electric field combinedly generates electrothermal forces which bring particles on the hotspot via toroidal vortex. Although REP removes most the limitations of the existing methodologies, it suffers from the requirement of high power budget, complications of implementing highly focused laser beam, and lack of ease.²⁶ A large amount of thermal energy ($\sim 85\%$) was wasted from the system,²⁷ which reveals the certain drawback of high energy loss. The system is not self-contained since the laser source is used externally.

Recently, we have demonstrated an alternative method of REP to manipulate colloidal particles continuously on a microfluidic chip. Our design system uses parallel plate electrodes similar to REP.²⁶ However, the technique does not necessitate externally adopted laser source to generate the thermal field. Instead, a simple change in chip design enables the non-uniform thermal field. Here, a thin insulating layer with a drilled narrow hole is attached on the bottom electrode. A non-uniform electric field was generated when the electric field penetrates through the hole. As a result, induced Joule heating generates a sharp temperature gradient which induces necessary gradients in electric properties to induce mobile charges for fluid flow. Therefore, the non-uniform electric field and non-uniform thermal field induce electrothermal forces to generate strong vortices bringing microparticles on the hotspot. Concentrating and patterning of the microparticles were shown in an energy-efficient way. The system is self-contained as all the components are embedded on a microfluidic chip. The Joule heating-induced particle manipulation addresses the limitations of the laser-induced REP. Also, Joule heating-induced electrothermal flow has numerous application for fluid pumping,^{28,29} mixing of analytes,^{30,31} controlling two-phase flow^{32,33}, etc.

The observations from the previous study intuitively highlight crucial features of particle manipulation which may be employed in a bio-assay system for efficient manipulation of cells. However, the biocompatibility of this method is not yet considered. Due to the motility of the biological objects, manipulation of bioparticles using Joule heating-induced REP may be complicated in comparison with colloidal particles. In this article, we explore the details study of biocompatibility of the Joule heating-induced REP via manipulation of various cells. The concentration and patterning into different designs of the cells using this method establish the biocompatibility of this technique for the efficient and effective performance of a bioassay system.

2. Materials and methods

2.1. Device fabrication

The device consisted of two parallel plate electrodes separated by a spacer (Figure 1). The indium-tin-oxide (ITO, thickness 150 nm) coated glass substrates (thickness 1.1 mm) were used as the top and bottom electrodes. The bottom electrode was covered with a layer of cello tape (thickness: $40\ \mu\text{m}$) which acted as an insulating layer. Thereafter, a narrow hole (hydraulic diameter $\sim 50\ \mu\text{m}$) was drilled at the middle of the insulating layer taking

precaution to not damage the ITO coating over the glass substrate. Both top and bottom electrodes were then integrated to fabricate the device with double-sided adhesive tape (thickness: 35 μm) acting as the spacer. The electrodes were connected to an AC function generator (33250A, Agilent) accompanied by a signal voltage amplifier (9200, High Voltage Wide Band Amplifier).

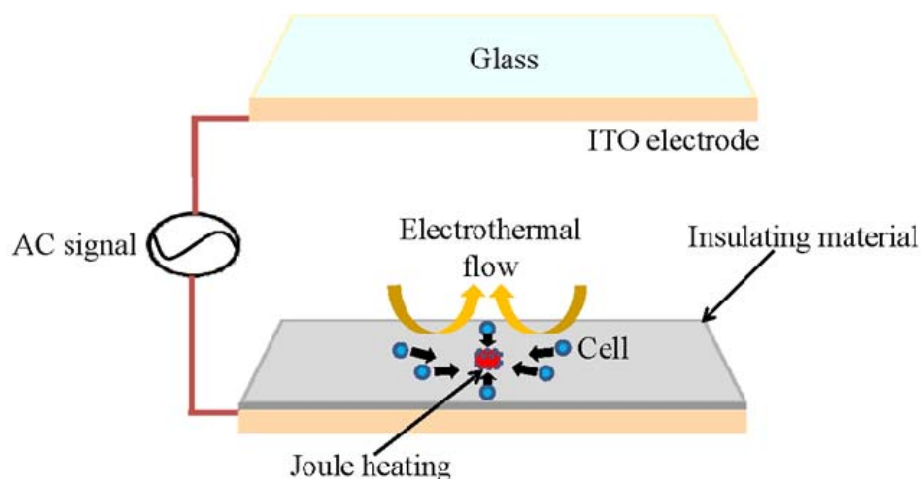


FIG. 1. Schematic illustration of the electrothermal flow for cell concentrating and patterning. AC electric field was applied across the parallel electrodes which result in Joule's heating at the narrow opening in the bottom electrode (zone of peak temperature). Thermal field and electric field, together, generate an electrothermal vortex which concentrates the suspended cell at the zone of peak temperature.

2.2. Cell culture and preparation

2.2.1. Bacterial cells

In the experiments, GFP-expressing bacteria (diameter: 0.8 μm , length: 2-3 μm) were used. For this, the GFP sequence was cloned in pet28a bacterial plasmid vector and transformed in *E. coli*. (BL21 strain) using a standard calcium chloride method. The transformed colonies were grown and selected on Luria agar plates containing kanamycin (400ug/ml). Prior to experimentation, the bacterial cultures were grown in Luria broth (Himedia, India) supplemented with kanamycin (400ug/ml) and IPTG (0.5 mM) for overnight at 37 °C under mild shaking conditions. Then, the cells were pelleted using centrifugation, washed twice with buffer solution (conductivity, $\sigma \sim 0.043$ S/m, isotonic low conductivity sucrose/dextrose buffer containing 8.3% sucrose and 0.3% dextrose prepared in injection water (SuperAmp[®], Otsuka)), and resuspended in the same buffer as per the desired concentration

2.2.2. Yeast cells

To prepare the yeast cells (strain BY4741, diameter: 3-4 μm), the cells were grown in Yeast Extract–Peptone–Dextrose media (Himedia, India) for 24 h at 30 °C under mild shaking conditions. The cells were then harvested, pelleted and washed with phosphate buffered saline (PBS, pH 7.4) and stained with CellTracker[™] Red (Life Technologies,

prepared in PBS) for 30 min at 30 °C. Thereafter, the cells were washed once with PBS, followed by two washes with buffer (conductivity, $\sigma \sim 0.043$ S/m), and resuspended in the same buffer as per the desired concentration.

2.3. Cell patterning methodology

The solution with suspended cells was injected between the electrodes. The electric field was then applied to actuate the cell motion. Induced internal Joule heat causes temperature gradients which would further induce inhomogeneities in the dielectric properties of the buffer solution. These induced electrothermal forces generate a directional fluid motion which would induce motion in the cells present in the nearby vicinity. Flow observation was carried out using an inverted microscope (IX71, Olympus) whereas images were captured using a CCD camera (ProgRes MF^{cool}) and 10X and 40X objective lens. To characterize the phenomenon of particle trapping and patterning, micro-particle image velocimetry (μ PIV) analysis was carried out. The experiments were performed for a fixed frequency of 500 kHz and a varying voltage of 3.54-9 V (root mean square). A voltage below 3.54 V was insufficient to induce significant cell trapping, while at a voltage above 9 V, electrolytic reactions were observed. Notably, electrolysis reactions were also evident at frequency range below 100kHz. The consequences of electrolytic reaction which depends on applied voltage and frequency of the AC signal are discussed in our previous work.²⁶

2.4. Theoretical basis

When electric field is applied into the system, potential (φ) will be distributed in accordance with ^{34,35} $\nabla \cdot (\sigma \nabla \varphi) = 0$, where σ is the electrical conductivity. The externally applied AC electric field causes heat generation in the bulk fluid domain. This heat source, also known as Joule heat, causes temperature distribution as evident from the energy equation

$$\rho C_p \frac{DT}{Dt} = \nabla \cdot (k \nabla T) + \sigma |\mathbf{E}|^2, \quad (1)$$

where C_p is the specific heat and k is the thermal conductivity. $\sigma |\mathbf{E}|^2$ is the Joule heat. ρ is the density of the buffer solution.

The velocity field is characterized by the Navier-Stokes equation. The present analysis deals with an electric field driven actuation mechanism where the thermal field has a strong effect to cause the electrothermal forces. Electrothermal forces are added in the Navier-Stokes equation and the whole equation can be written as:

$$\rho \frac{D\mathbf{V}}{Dt} = -\nabla p + \nabla \cdot [\mu (\nabla \mathbf{V} + \nabla \mathbf{V}^T)] + \mathbf{F}_E, \quad (2)$$

Here, \mathbf{V} is the fluid velocity and μ is the viscosity of the fluid. The time-averaged electrothermal force is expressed by ^{36,37}

$$\mathbf{F}_E = \frac{1}{2} \text{Re} \left[\frac{\sigma \varepsilon (\alpha - \beta)}{\sigma + i\omega \varepsilon} (\nabla T \cdot \mathbf{E}) \mathbf{E}^* - \frac{1}{2} \varepsilon \alpha |\mathbf{E}|^2 \nabla T \right], \quad (3)$$

where Re is the real part of []. \mathbf{E} is the electric field and \mathbf{E}^* is the complex conjugate. ω is the frequency of the AC signal. ε is the permittivity of the fluid. α and β are $(1/\varepsilon)(\partial \varepsilon / \partial T)$

and $(1/\sigma)(\partial\sigma/\partial T)$, respectively. The first term of the right-hand side of the Eq. (3) is known as the Coulomb force whereas, the second term is the dielectric force of the electrothermal forces. From the equation, it is also clear that temperature gradients cause the local variations in electrical properties.

In addition to the electrothermal forces, some other electrical forces, such as dielectrophoretic force, electroosmotic force and electrostatic interactions simultaneously interact with van der Waals attraction force near the drilled hole. As a result, a net force prevails in the hotspot area, which effectively acts as a holding force for the cells and causes their aggregation on the bottom electrode. Specifically, DEP which is generated due to the integration between the non-uniform electric field and induced dipole on the polarized cells dominates over other electrical forces near the hole. At this location, the electric field is highly non-uniform and interaction between the particles and electric field is high.²⁶ Notably, buoyancy force cannot influence electrothermal velocity for such a configuration where characteristics length scale $l_c \sim 100 \mu\text{m}$ as they come into play for $l_c > 1000 \mu\text{m}$.³⁸

3. Results and discussion

The directional flow from surrounding to the hotspot site driven by Joule's heating-induced (internal heat generation) electrothermal mechanism is a multiphysics problem where electric, thermal and flow fields are coupled simultaneously. The buffer solution in the system completes the circuit between the parallel plate electrodes. Upon application of the AC electric field, a non-uniform field get generated with the maximum field strength at the site of drilled hole (at the bottom electrode) which sharply decreases as the function of distance. Notably, electric field and electrical conductivity together contribute in the Joule heating, however, the conductivity of the domain remains uniform; thus, the thermal field generated resembles the shape of electric field. In the thermal field, a sharp gradient in temperature is occurs at the plane just above the insulating layer with the highest temperature located at the centre of the liquid placed above the hole and the local temperature sharply decreases with the distance. As a result, temperature-sensitive electrical properties including conductivity and permittivity are get influenced by the generated temperature gradient especially in the particles present around the hotspot. Since the conductivity of the solution maintains the current flow mobile charges are induced into the system to main the current continuity perturbed by the conductivity gradient. On the other hand, mobile charges are also induced by the influence of the gradient of permittivity since the charge is a function of permittivity and gradient of permittivity. Therefore, the gradient of permittivity and conductivity together generate mobile charges. The flow of the mobile charges, and hence, the flow of solution and particles are generated according to variation of temperature. Thus, particles move from the surrounding to hotspot site.

One important point to be mentioned here is that the thermal filed which is the source of electrothermal forces may affect the cell life and cell activity. It was reported that the functionalities of the biological samples are spoiled above a temperature rise of 10K.³⁹ Considering this threshold value of temperature as limiting case our design Joule heating-induced cell manipulation is not affected by the thermal field since for such a scenario temperature rise is well below of 10 K.²⁶ The important fact is that the temperature gradient

causes the variation in electrical properties to induce mobile charges, not the absolute temperature. The chip is design accordingly to obtain a highly nonuniform temperature without rising absolute temperature much. Also, there are many studies which represented the electrothermal actuation to handle biofluid, bioreagent.^{40–45}

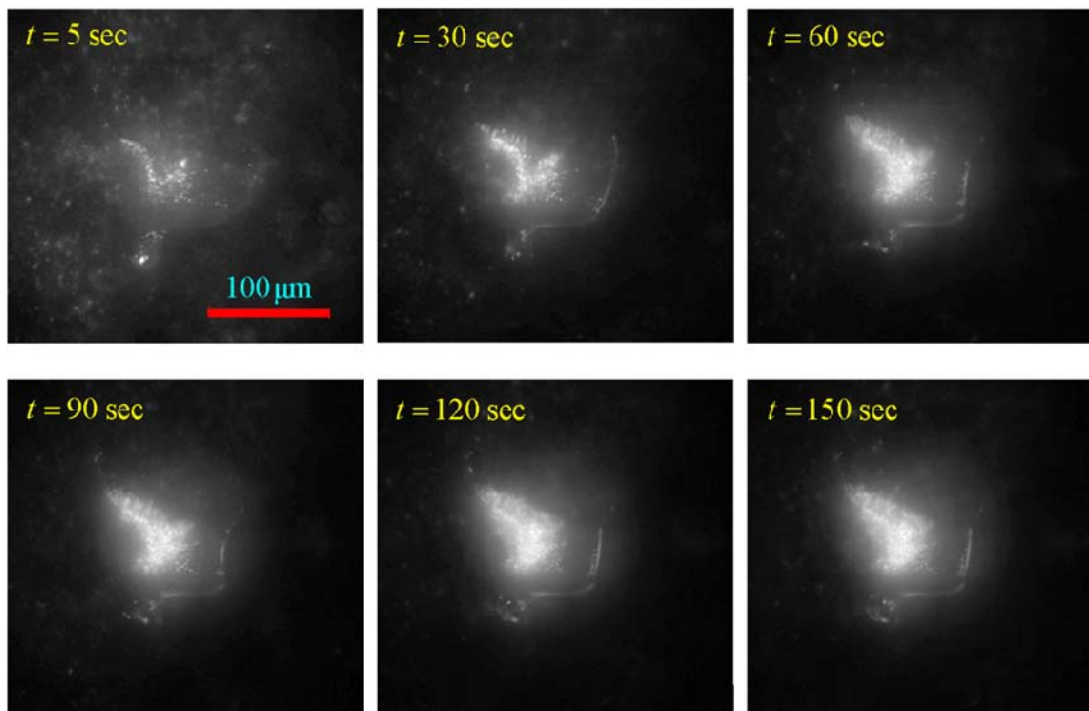


FIG. 2. Time instances ($t = 5 \text{ sec}$, $t = 30 \text{ sec}$, $t = 60 \text{ sec}$, $t = 90 \text{ sec}$, $t = 120 \text{ sec}$ and $t = 150 \text{ sec}$) of images showing *E. coli* concentrating process. After a rapid aggregation in $t = 5 - 80 \text{ sec}$ cell aggregation shows gradual accumulation in the time interval of $t = 80 - 120 \text{ sec}$ and almost negligible accumulation for the rest of the time. The applied voltage is 7.08 V .

The aggregation of the *E. coli* bacteria is presented in Fig. 2 by highlighting image sequences for an applied voltage of 7.08 V (root mean square). Cell trapping process starts as soon as the electric field is applied. Since the thermal field is produced using the electric field itself electrothermal actuation begins once the electric field is imposed on the system. However, laser-induced REP for bioassay system requires electric field and laser beam simultaneously.¹⁸ There may be a delay to commence the manipulation process because to induce the thermal field by laser time is elapsed. Although electrothermal flow brings the cells from the surrounding to the hotspot at the plane shown in the figure, an outward electrothermal flow must prevail at the other plane to maintain the mass conservation of the solution. The buffer solution cannot be stored anywhere in the system. In the absence of other force to trap the cells, the aggregation will not happen. However, a net force including dielectrophoresis on the trapping region holds the cells arrived owing to electrothermal flow. Therefore, electrothermal mechanism transports the cells to the trapping location and holding force traps the cells. For the first row of the images shows a rapid change in the number of trapping cells while this change is slow for the second row of images. The electric field

strength is not changed with time and also the thermal field is not altered. Hence, electrothermal flow always presents and works as a cell carrier. However, the dielectrophoresis force which is the dominating force of holding force drastically falls from the hole location. The region over which the cell accumulation appears is rapidly filled by the stack of cluster cells. After sometimes aggregation rate sharply decreases due to lack of holding force at location distanced from the drilled hole.

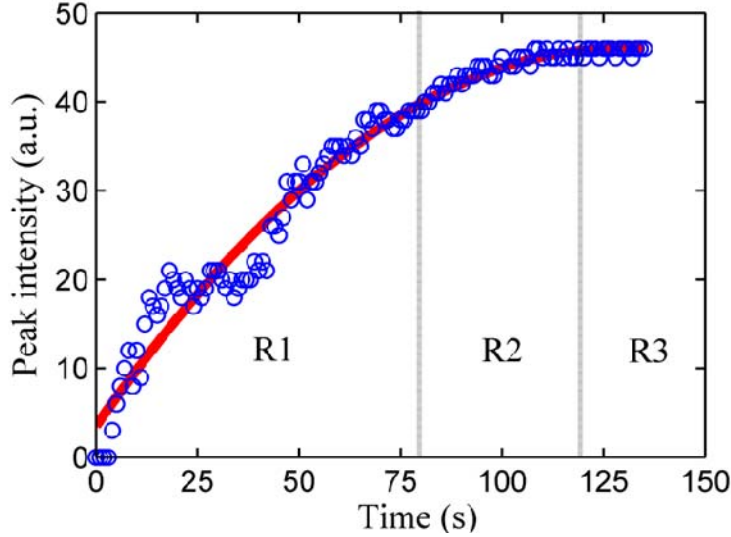


FIG. 3. (a) Increase in maximum fluorescence intensity with time showing rate of aggregation of *E. coli* bacteria. The aggregation process is divided into three regions: R1 (rapid aggregation), R2 (slower aggregation), and R3 (no significant aggregation). The applied voltage is 7.08 V.

We show the time vs fluorescent intensity plot in Fig. 3 for further assessment of the cell concentrating process. The increase in the maximum intensity of the fluorescent with respect to the fluorescent intensity at time $t = 0$ sec is highlighted in the figure. Maximum fluorescent intensity first increases sharply up to $t \sim 80$ sec and then mildly increases up to $t \sim 120$ sec. After saturation of the aggregation process variation of maximum intensity shows a plateau ($t > 120$ sec). At the initial stage of the aggregation step, the trapping region is completely blank and all the forces in the system work strongly. However, when the trapping region is filled with cells holding force shows the inability to further trap the bioparticles. Another reason may also be stated that after significant concentration of the cells the concentration of the cells in the domain becomes commodious. As a result, the chance of further aggregation becomes less. For clear visualization the area of time vs intensity is divided into three regions, R1: domain of rapid change in fluorescent intensity; R2: domain of meekly change in fluorescent intensity and R3: domain of negligible change in fluorescent intensity.

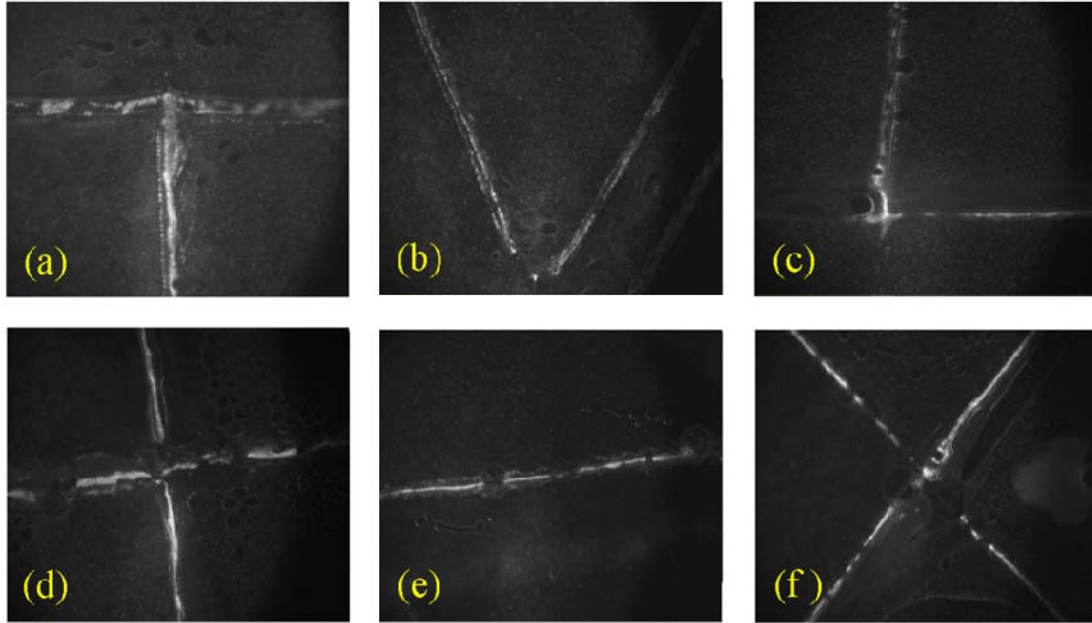


FIG. 4. Different patterns formation of *E. coli* bacteria: (a) “T”, (b) “V”, (c) “L”, (d) “+”, (e) “-”, and (f) “x” for $\phi = 7.08$ V. The widths of the different geometries are in the range of 50-200 μm . The designs of the pattern follow the opened section on the bottom electrode.

The important aspect of the present technique is the ability to form different cell patterns in an easy way. *E. coli* drives its body through the rotation of flagella motors attached to the cell membrane. Depending on the direction of rotation *E. coli* moves along a straight line or rotates at the same place. Alternation of the direction of rotation influences the overall motion. Such motions of *E. coli* were found in our experiments. However, when the electric field is applied the rotational axis is aligned with the electric field due to the larger force of the electrothermal effects. Further, different patterns of the *E. coli* are formed by designing different opening structures on the bottom electrode. Previously, it was seen that the cells are concentrated at the location of peak temperature which is observed in the drilled area. Therefore, it is expected that the different structures of the Joule heating pattern made by the opening the bottom electrode can generate different shapes of the clustering cells. Different shapes of the aggregated cells, such as letters “T”, “V”, “L” and signs “+”, “-” “x” are generated (Fig. 4) by resembling the shapes of the pattern formed on the insulating layer. Cell patterning shown here has an important application in tissue engineering for cell culture, specifically during the growth phase of tissue to preserve cell viability.

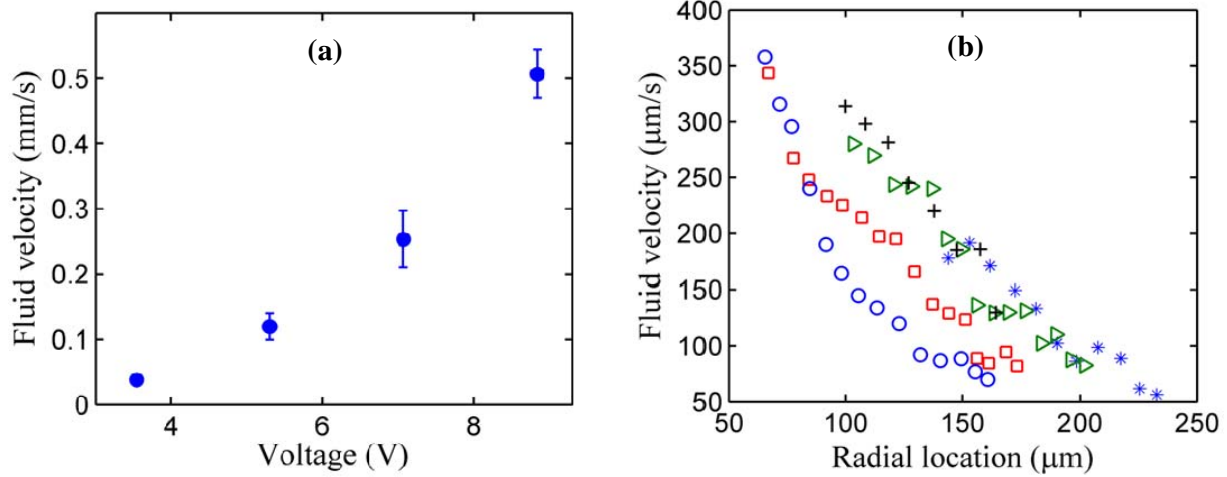


FIG. 5. (a) Plot of voltage vs mean velocity and (b) variation of local velocity with radial distance from the trapping region for $\phi = 7.08$ V. Mean velocity sharply increases with voltage as electric field strength and Joule heating both increases with voltage. Due to the rapid drop in the electric field from the trapping region local velocity shows a sharp drop near that region.

There are various parameters which directly or indirectly influence the cell concentrating and patterning processes. The voltage of the imposed AC signal affects the cell trapping deeply because generated Joule heating which solely takes the role of movement of the cells towards a target location is induced due to the applied voltage. In order to reveal the important features of underlying flow physics of cell trapping controlled by voltage the mean velocity data with voltage and spatially varying local velocity are presented in Fig. 5. The mean velocity is evaluated at a distance of 75-100 μm from the trapping region and local velocity is taken at a voltage of 7.08 V. The mean velocity shows a rapid increase in magnitude with increasing voltage. Previously, it was described that electric field strength and temperature gradients combinedly affect the cell velocity and trend of variations are incremental for both effects. Therefore, it is expected that cell velocity increases rapidly with applied voltage. To characterize the dependency of the velocity with voltage it was reported that ideally fluid velocity varies with fourth power of the signal voltage ($V \sim \phi^4$).²⁶ This is due to fact that electrothermal force is proportional with square of electric field and varies linearly with temperature gradient, and finally temperature gradient varies with square of the electric field strength ($F_E \sim E^2 \nabla T$, $\nabla T \sim E^2$). However, Experimentally obtained data of voltage vs velocity shows an index of 2.93 ($V \sim \phi^{2.93}$), which is lower than the theoretically predicted index. The slight deviation from the ideal value may be attributed with the cause that expects electrothermal forces, other electric forces including van der Waals force interact with ET forces near the trapping area. Consequently, the driving force (ET force) which brings the cells towards the trapping region becomes weak slightly and theoretically dependence index differs from the experimentally obtained value. However, a variation of the velocity field with voltage is advantageous as compared to Joule-heating induced REP because for such a scenario produced velocity squarely depends with signal voltage.²⁷

Local velocity sharply drops near the aggregation spot and then gradually as it distanced from the spot (Fig. 5(b)). As seen before the fluid velocity strongly depends on the

electric field strength. Since the electric field sharply reduces the temperature gradient and electrothermal forces decrease rapidly from the trapping region. Hence, local velocity shows a rapid decrease in velocity magnitude near the trapping region and then meekly decreases. Some other parameters, such as the area of the drilled hole, the distance between the two electrodes have significant influence of cell trapping process. The conclusions drawn from the experiments are similar to our previous publication.²⁶

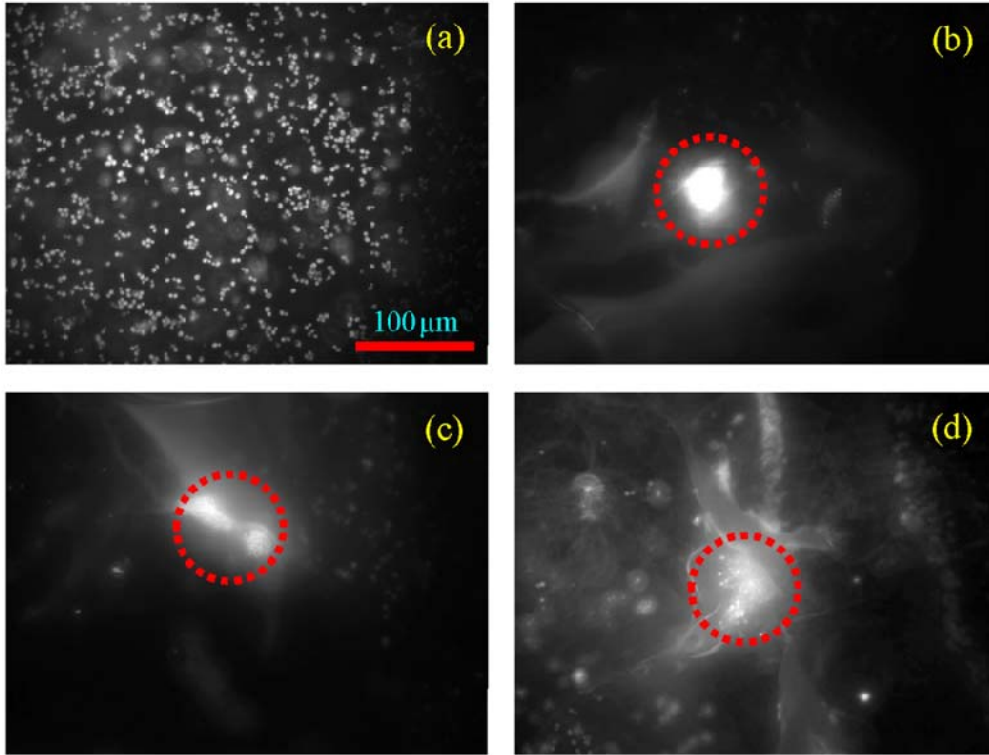


FIG. 6. (a) Distribution of the yeast cells without an electric field. Concentration of the yeast cells for $\varphi = 7.08$ V ((a)-(c)). The hydraulic diameter of the drilled hole is 50-100 μm . The images are shown at $t = 50$ sec from the start of the aggregation process.

To expand the development in the biocompatibility of Joule heating-induced REP we performed the experiments for yeast cell. We show the aggregation of yeast cells in Fig. 6 for an applied voltage of 7.08 V. Fig. 6(a) shows the distribution of yeast cells without applying the electric field while Figs.6(a)-(c) highlights the results of cell aggregation in three different sets of experiments. For all cases, we obtain aggregation of yeast. The present technique can be applied for wide ranges of bioparticles since the electrothermal forces arise from the interactions between electric and thermal field and not utilizing interactions between bioparticle and electric fields.

4. Conclusions

We have shown a novel Joule heating-induced continuous cell concentrating and patterning method that exploits the interplay between the non-uniform electric field and non-uniform thermal field. Using an alternating current electric field with a simple design of the microfluidic chip the technique enables trapping of different bio-objects, such as *Escherichia*

coli bacterial cell and yeast cell with high throughput in an efficient way. Further, the method does not necessitate the pre-treatment of the biosamples. The electrokinetic processor developed in the present study has the ability to enhance reproducibility and response of biosensors by allowing simple and fast cell analysis. With several important advantages, such as operation at low power, high speed, high-accuracy, simplicity in design the technique can be applied in different applications ranging from tissue engineering, drug screening, microarray to cell studies.

References

- ¹ R. Edmondson, J.J. Broglie, A.F. Adcock, and L. Yang, *Assay and Drug Development Technologies* **12**, 207 (2014).
- ² N. Kramer, A. Walzl, C. Unger, M. Rosner, G. Krupitza, M. Hengstschläger, and H. Dolznig, *Mutation Research/Reviews in Mutation Research* **752**, 10 (2013).
- ³ J. Nilsson, M. Evander, B. Hammarström, and T. Laurell, *Analytica Chimica Acta* **649**, 141 (2009).
- ⁴ B. Guillotin and F. Guillemot, *Trends in Biotechnology* **29**, 183 (2011).
- ⁵ L. Kang, B.G. Chung, R. Langer, and A. Khademhosseini, *Drug Discovery Today* **13**, 1 (2008).
- ⁶ B.M. Taff and J. Voldman, *Analytical Chemistry* **77**, 7976 (2005).
- ⁷ S. Kar, T.K. Maiti, and S. Chakraborty, *Analyst* **140**, 6473 (2015).
- ⁸ K. Chaudhury, U. Ghosh, and S. Chakraborty, *International Journal of Heat and Mass Transfer* **67**, 1083 (2013).
- ⁹ S. Chakraborty, *Lab on a Chip* **5**, 421 (2005).
- ¹⁰ K. Ino, H. Shiku, F. Ozawa, T. Yasukawa, and T. Matsue, *Biotechnology and Bioengineering* **104**, 709 (2009).
- ¹¹ J.R. Rettig and A. Folch, *Analytical Chemistry* **77**, 5628 (2005).
- ¹² F. Arai, C. Ng, H. Maruyama, A. Ichikawa, H. El-Shimy, and T. Fukuda, *Lab on a Chip* **5**, 1399 (2005).
- ¹³ X. Wang, S. Chen, M. Kong, Z. Wang, K.D. Costa, R.A. Li, and D. Sun, *Lab on a Chip* **11**, 3656 (2011).
- ¹⁴ N. Pamme and A. Manz, *Analytical Chemistry* **76**, 7250 (2004).
- ¹⁵ X. Hu, P.H. Bessette, J. Qian, C.D. Meinhardt, P.S. Daugherty, and H.T. Soh, *Proceedings of the National Academy of Sciences* **102**, 15757 (2005).
- ¹⁶ I. Cheng, V.E. Froude, Y. Zhu, H. Chang, and H. Chang, *Lab on a Chip* **9**, 3193 (2009).
- ¹⁷ B.A. Nestor, E. Samiei, R. Samanipour, A. Gupta, A. den Berg, M.D. de Leon Derby, Z. Wang, H.R. Nejad, K. Kim, and M. Hoorfar, *RSC Advances* **6**, 57409 (2016).
- ¹⁸ J.-S. Kwon, S.P. Ravindranath, A. Kumar, J. Irudayaraj, and S.T. Wereley, *Lab on a Chip* **12**, 4955 (2012).
- ¹⁹ L.-C. Hsiung, C.-H. Yang, C.-L. Chiu, C.-L. Chen, Y. Wang, H. Lee, J.-Y. Cheng, M.-C. Ho, and A.M. Wo, *Biosensors and Bioelectronics* **24**, 869 (2008).
- ²⁰ C. Iliescu, G. Xu, W.H. Tong, F. Yu, C.M. Bualan, G. Tresset, and H. Yu, *Microfluidics and Nanofluidics* **19**, 363 (2015).
- ²¹ K.-C. Wang, A. Kumar, S.J. Williams, N.G. Green, K.C. Kim, and H.-S. Chuang, *Lab Chip* **14**, 3958 (2014).
- ²² H. Morgan, M.P. Hughes, and N.G. Green, *Biophysical Journal* **77**, 516 (1999).
- ²³ V. Velasco and S.J. Williams, *Journal of Colloid and Interface Science* **394**, 598 (2013).
- ²⁴ I.R. Perch-Nielsen, D.D. Bang, C.R. Poulsen, J. El-Ali, and A. Wolff, *Lab on a Chip* **3**, 212 (2003).
- ²⁵ S.J. Williams, A. Kumar, and S.T. Wereley, *Lab on a Chip* **8**, 1879 (2008).

- ²⁶ G. Kunti, J. Dhar, A. Bhattacharya, and S. Chakraborty, *Biomicrofluidics* **13**, 014113 (2019).
- ²⁷ S.J. Williams, A. Kumar, G. Green, and S.T. Wereley, *Nanoscale* **1**, 133 (2009).
- ²⁸ A. Salari, M. Navi, and C. Dalton, *Biomicrofluidics* **9**, 014113 (2015).
- ²⁹ G. Kunti, J. Dhar, A. Bhattacharya, and S. Chakraborty, *Journal of Applied Physics* **123**, 244901 (2018).
- ³⁰ J.J. Feng, S. Krishnamoorthy, and S. Sundaram, *Biomicrofluidics* **1**, 024102 (2007).
- ³¹ G. Kunti, A. Bhattacharya, and S. Chakraborty, *Electrophoresis* **38**, 1310 (2017).
- ³² G. Kunti, A. Bhattacharya, and S. Chakraborty, *Physics of Fluids* **31**, 32002 (2019).
- ³³ G. Kunti, A. Bhattacharya, and S. Chakraborty, *Soft Matter* **13**, 6377 (2017).
- ³⁴ Castellanos A, *Electrohydrodynamics* (Springer, New York, 1998).
- ³⁵ F.J. Hong, F. Bai, and P. Cheng, *Microfluidics and Nanofluidics* **13**, 411 (2012).
- ³⁶ N.G. Green, A. Ramos, A. Gonzalez, A. Castellanos, and H. Morgan, *Journal of Electrostatics* **53**, 71 (2001).
- ³⁷ A. Ramos, H. Morgan, N.G. Green, and A. Castellanos, *Journal of Physics D: Applied Physics* **31**, 2338 (1998).
- ³⁸ A. González, A. Ramos, H. Morgan, N.G. Green, and A. Castellanos, *J Fluid Mech* **564**, 415 (2006).
- ³⁹ S. Lim, H. Park, E. Choi, and J. Kim, *Key Engineering Materials* **343**, 537 (2007).
- ⁴⁰ J. Wu, M. Lian, and K. Yang, *Applied Physics Letters* **90**, 234103 (2007).
- ⁴¹ Q. Yuan, K. Yang, and J. Wu, *Microfluidics and Nanofluidics* **16**, 167 (2014).
- ⁴² Q. Yuan and J. Wu, *Biomedical Microdevices* **15**, 125 (2013).
- ⁴³ R.H. Vafaie, H.B. Ghavifekr, H. Van Lintel, J. Brugger, and P. Renaud, *Electrophoresis* **37**, 719 (2016).
- ⁴⁴ Q. Lang, Y. Ren, D. Hobson, Y. Tao, L. Hou, Y. Jia, Q. Hu, J. Liu, X. Zhao, and H. Jiang, *Biomicrofluidics* **10**, 064102 (2016).
- ⁴⁵ J. Gao, M.L.Y. Sin, T. Liu, V. Gau, J.C. Liao, and P.K. Wong, *Lab on a Chip* **11**, 1770 (2011).